ACS APPLIED MATERIALS & INTERFACES

Research Article

www.acsami.org

Electrospun TiO_2 Nanofelt Surface-Decorated with Ag Nanoparticles as Sensitive and UV-Cleanable Substrate for Surface Enhanced Raman Scattering

Yong Zhao,[†] Lei Sun,[‡] Min Xi,[†] Quan Feng,[†] Chaoyang Jiang,*[,‡] and Hao Fong*[,†]

[†]Department of Chemistry and Applied Biological Sciences, South Dakota School of Mines and Technology, Rapid City, South Dakota 57701, United States

[‡]Department of Chemistry, University of South Dakota, Vermillion, South Dakota 57069, United States

Supporting Information

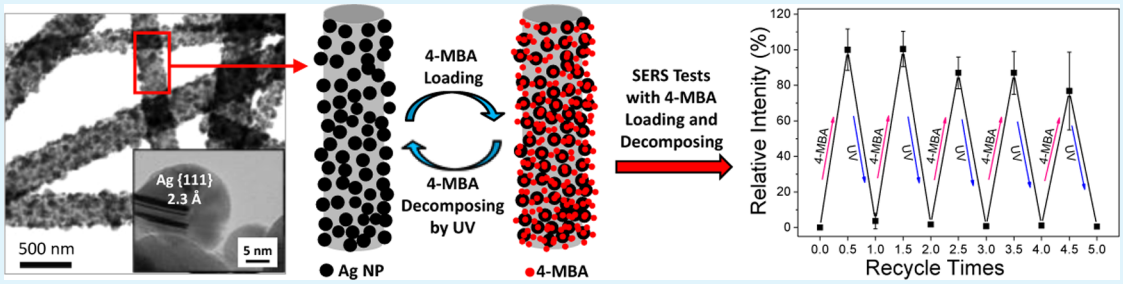

ABSTRACT: In this study, the free-standing electrospun nanofibrous mat (i.e., nanofelt) consisting of anatase-phase TiO_2 nanofibers with diameters of ~200 nm was prepared, and the nanofelt was subsequently surface-decorated with Ag nanoparticles via an electroless plating method. The sensitivity toward surface enhanced Raman scattering (SERS) and UV-cleanable property of electrospun TiO_2/Ag nanofelt were then investigated. In the SERS tests, the target analyte (i.e., 4-mercaptobenzoic acid, Rhodamine 6G, and 4-aminothiophenol) was first adsorbed onto the TiO_2/Ag nanofelt as the probe analyte; this was followed by the measurements of Raman intensity and SERS maps. Thereafter, the nanofelt adsorbed with target analyte was cleaned and regenerated/recovered upon UV irradiation in O_2-saturated water, and the removal of target analyte was attributed to photodegradation property of anatase-phase TiO_2. This study suggested that the electrospun TiO_2/Ag nanofelt would be promising as SERS-active substrate with UV-cleanable property for cost-effective and reproducible SERS applications.

KEYWORDS: *electrospinning, TiO_2, Ag nanoparticles, UV-cleaning, SERS*

1. INTRODUCTION

Surface-enhanced Raman scattering (SERS) has been widely investigated for ultrasensitive chemical and biological detections because of its capability of providing molecule-level information on analytes adsorbed on SERS-active substrates.[1−3] Noble metal nanostructures, particularly those made of Au and Ag, have shown excellent SERS activity/sensitivity because of their unique characteristics of localized surface plasmon resonance.[4−6] To further facilitate and broaden SERS applications, it is important to develop cost-effective and reusable nanostructured SERS substrates with controlled/desired morphologies and structures. Recently, new composite and/or hierarchically structured materials with high SERS activity/sensitivity have been designed and synthesized from nanostructured support materials together with noble-metal nanoparticles.[7,8] For example, Ko et al. prepared 3-dimensional Al_2O_3 membranes loaded with Au nanoparticles (Au NPs) and explored the SERS enhancement.[9] Zhai et al. synthesized Fe_3O_4 core/Au shell submicrometer structures with strong SERS-activity in the near-infrared range.[10] Zhang et al. reported that the Ag-graphene nanosheets with adjustable sizes and well-controlled densities of Ag NPs would be excellent SERS-active substrate.[11]

The technique of electrospinning provides a convenient approach for the fabrication of fibers with diameters typically in the range from tens to hundreds of nanometers (commonly known as electrospun nanofibers).[12,13] Recently, there have been several reports on the development of SERS-active substrates by attaching metal nanostructures (e.g., nanoparticles of Au and Ag) onto electrospun nanofibers via the methods such as drop-casting, sputter-coating, chemical reduction, and electroless plating.[14−20] For example, He et al. prepared electrospun poly(vinyl alcohol) (PVA) nanofibers embedded with Ag NPs as SERS-active substrate;[17] Au NPs/nanorods have also been successfully assembled into electrospun PVA nanofibers for SERS applications.[18,19] Lee et al. used the drop-casting method to obtain oriented Au nanorods on electrospun nanofibers with high SERS sensitivity.[20] However, most of the

Received: January 26, 2014
Accepted: April 1, 2014
Published: April 1, 2014

   dx.doi.org/10.1021/am5005859 | ACS Appl. Mater. Interfaces 2014, 6, 5759−5767

SERS-active substrates cannot be easily cleaned and regenerated/reused after SERS analyses; this is inconvenient and is not cost-effective because of the high costs of noble metals (e.g., Au and Ag).

It is well-known that titanium(IV) oxide (TiO_2) in its crystalline phase/structure of anatase is a UV-responsive (<400 nm) semiconductor, and it is highly active toward the photochemical degradation of organic compounds.[21−25] The oxidation−reduction capability of various crystal facets of anatase TiO_2 has been investigated, and the {101} facet is considered the most responsible for photocatalytic activities.[26,27] The photochemical degradation of anatase TiO_2 is a typical oxidative process attributed to oxidizing radical species, such as $^{\bullet}O_2^-$ and $^{\bullet}OH$. Upon irradiated under UV light, the excited TiO_2 crystallites will reduce the dissolved/adsorbed molecular oxygen into a superoxide radical, which will then generate highly active oxidative species, such as $^{\bullet}O_2^-$ and $^{\bullet}OH$. These oxidative species can subsequently lead to the degradation of organic compounds adsorbed on the surfaces of TiO_2.[22−25] Recently, there have been several reported studies on the metal−semiconductor hierarchically structured materials as cleanable/recyclable SERS substrates (especially on the TiO_2-based SERS substrates),[28−33] and the results have clearly demonstrated the excellent performance and remarkable reusability of the TiO_2-based SERS substrates. During the evaluation of those nanostructured SERS substrates, however, extra procedures are typically required for the sample preparation, treatment, and collection. As a further step, it is important to make the cleanable/recyclable TiO_2-based SERS substrates large, uniform, and free-standing, since such SERS substrates are critical for the practical applications in molecular detection and ultrasensitive sensing.

In this research, the free-standing overlaid nanofibrous mat (i.e., nanofelt) consisting of anatase-phase TiO_2 nanofibers with diameters of ∼200 nm was first prepared by the technique of electrospinning followed by the pyrolysis in air at 500 °C, as schematically shown in Figure 1. Ag NPs were then decorated

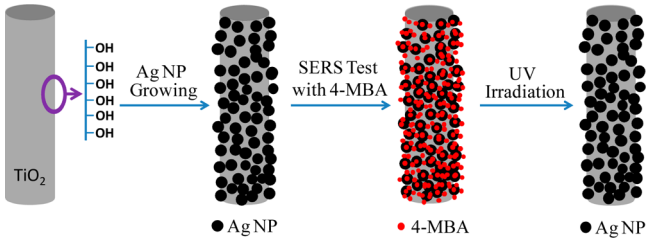

Figure 1. Schematic representation showing the electrospun TiO_2 nanofiber surface-decorated with Ag NPs for SERS detection of 4-MBA with UV-cleanable property.

onto electrospun TiO_2 nanofelt via the electroless plating method. For the target analytes, 4-mercaptobenzoic acid (4-MBA), rhodamine 6G (R6G), and 4-aminothiophenol (4-ATP) were selected to study the SERS sensitivity of electrospun TiO_2/Ag nanofelt.[34] During the SERS tests, the target analyte (i.e., 4-MBA, R6G, and 4-ATP) was adsorbed onto the TiO_2/Ag nanofelt as the probe analyte; and this was followed by the measurement of Raman intensity and SERS maps. Thereafter, the electrospun TiO_2/Ag nanofelt adsorbed with target analyte was cleaned and fully regenerated/recovered upon UV irradiation of the nanofelt to decompose/remove the target analyte. This research indicated that the electrospun TiO_2/Ag nanofelt would be promising as SERS-active substrate with UV-cleanable property for cost-effective and reproducible SERS applications.

2. EXPERIMENTAL SECTION

2.1. Materials. Titanium(IV) *n*-butoxide (TNBT), polyvinylpyrrolidone (PVP, M_w = 1 300 000), *N*,*N*-dimethylformamide (DMF), isopropanol (IPA), ethanol, acetic acid (HAc), potassium hydroxide (KOH), and ammonium hydroxide (NH_4OH) were purchased from Sigma-Aldrich (St. Louis, MO) and used without further purification.

2.2. Preparation of Electrospun TiO_2 Nanofelt. Prior to electrospinning, 1.25 g of PVP was dissolved in a mixture solvent of 3.88 g of DMF and 1.38 g of IPA, while 2.5 g of TNBT was mixed with 2.5 g of IPA, 2.5 g of DMF, and 1.0 g of HAc. The solutions of PVP and TNBT (8.3 and 16.7 wt % in the final spin dope, respectively) were then mixed together followed by being stirred for 24 h. Thereafter, the spin dope was filled into a 30 mL BD Luer-Lok tip plastic syringe having an 18 gauge 90° blunt-end steel needle. The electrospinning was carried out at 15 kV by using an ES30P high voltage supply (Gamma High Voltage Research, Inc.), and the feed rate was maintained at 1.0 mL/h by using a KDS syringe pump (KDS 200, KD Scientific Inc.). Electrospun nanofibers were collected on the electrically grounded aluminum foil that covered a laboratory-produced roller with diameter of ∼25 cm, and the distance between the aluminum foil and the tip of steel needle was set at ∼25 cm. After electrospinning, the nanofibrous mat was carefully peeled off from the aluminum foil, sandwiched between two ceramic plates (with size being 5 × 11 cm), and placed in a Lindberg 54453 Heavy Duty Tube Furnace. The following was the pyrolysis procedure to prepare the electrospun TiO_2 nanofelt: (1) increasing the temperature from 25 to 180 °C at 1.5 °C/min, (2) holding the temperature at 180 °C for 2 h, (3) increasing the temperature to 350 °C at 1.5 °C/min, (4) holding the temperature at 350 °C for 2 h, (5) increasing the temperature to 500 °C at 1.5 °C/min, (6) holding the temperature at 500 °C for 3 h to completely burn/remove organic components in the fibers and to allow TiO_2 to crystallize, and (7) naturally cooling off to room temperature. A constant flow of air was maintained through the furnace during the pyrolysis. Note that this pyrolysis profile is essential to acquire the free-standing anatase-phase TiO_2 nanofelt.

2.3. Surface-Decoration of Ag NPs on Electrospun TiO_2 Nanofelt. Surface-decoration of Ag NPs was carried out via the electroless plating method as reported before.[35] Prior to surface-decoration, the Tollen's reagent consisting of two parts was prepared. For making the first part, 15 M NH_4OH solution was added into 10 mL of 0.05 M $AgNO_3$ solution dropwise until the brown precipitate disappeared under the stirring condition; subsequently, 5 mL of 0.8 M KOH solution was added into the system, resulting in the formation of brown precipitate; thereafter, additional 15 M NH_4OH solution was added in dropwise until the system became clear and colorless again. The second part was 1 mL 0.12 M dextrose aqueous solution. The Tollen's reagent was prepared by mixing the two parts for 20 s under the stirring condition. Electrospun TiO_2 nanofelt was then immersed in the Tollen's reagent for electroless plating of Ag with reaction periods set at 1, 3, 10, and 20 min, respectively. The resulting TiO_2/Ag nanofelts (denoted hereafter as TiO_2/Ag-1 min, TiO_2/Ag-3 min, TiO_2/Ag-10 min, and TiO_2/Ag-20 min) were finally rinsed with distilled water for several times and then dried in air before morphological/structural characterizations and SERS evaluations.

2.4. Morphological and Structural Characterizations. A Zeiss Supra 40VP field-emission scanning electron microscope (SEM) was employed to examine the morphological structures of different nanofelts. The TiO_2/Ag-1 min, TiO_2/Ag-3 min, TiO_2/Ag-10 min, and TiO_2/Ag-20 min nanofelts were further characterized by a JEOL JEM-2100 transmission electron microscope (TEM). X-ray diffraction (XRD) patterns were acquired from a Rigaku Ultima Plus X-ray diffractometer operating at 40 kV and 90 mA with the Cu Kα radiation (wavelength λ = 0.154 nm). The XRD profiles were recorded from 10° to 70° with the scanning speed of 2 deg/min.

dx.doi.org/10.1021/am5005859 | ACS Appl. Mater. Interfaces 2014, 6, 5759−5767

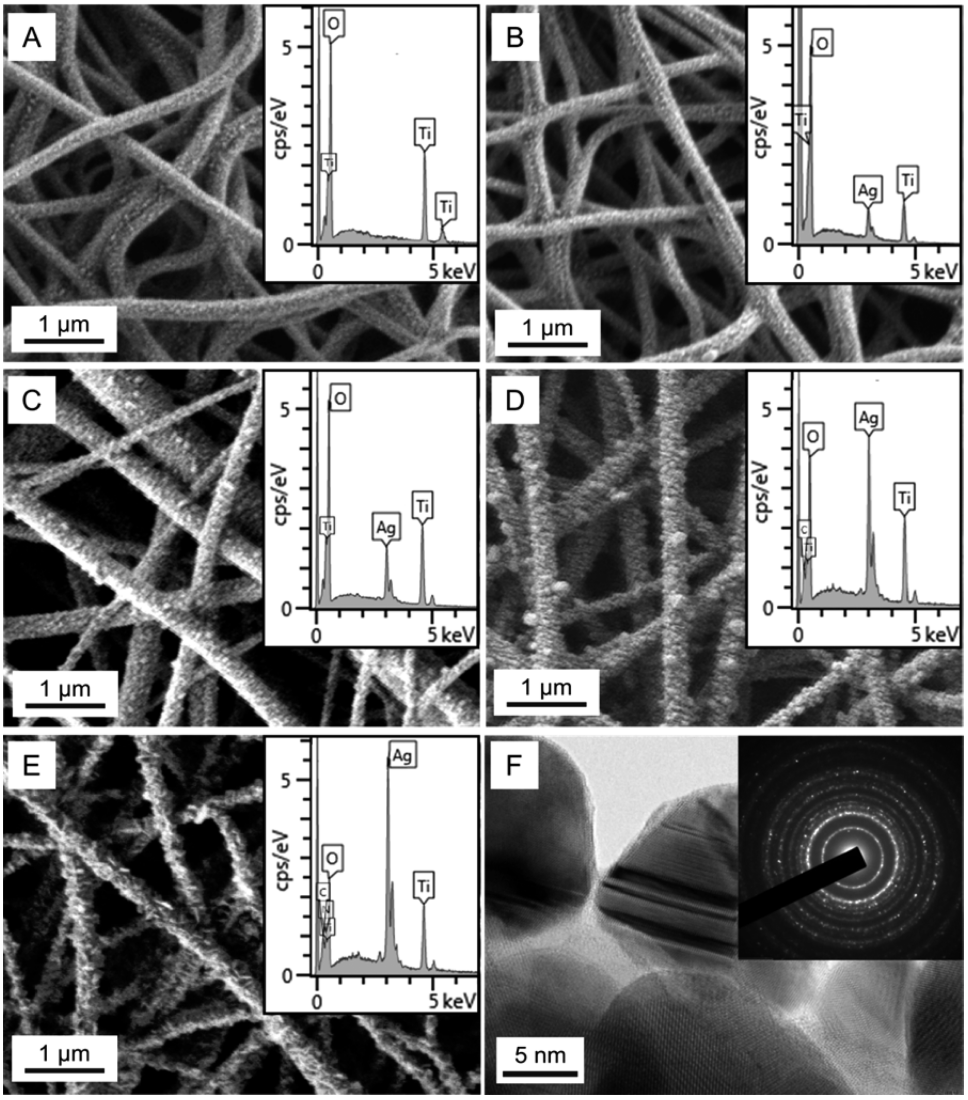

Figure 2. Representative SEM images showing the morphological structures of different nanofelts: (A) TiO_2, (B) TiO_2/Ag-1 min, (C) TiO_2/Ag-3 min, (D) TiO_2/Ag-10 min, and (E) TiO_2/Ag-20 min. TEM images of TiO_2/Ag-10 min nanofelt (F). The insets in images A, B, C, D, and E are EDS results of the corresponding nanofelts, respectively. The inset in image F shows the typical electron diffraction pattern acquired from TiO_2/Ag-10 min nanofelt.

2.5. SERS Measurements. SERS spectra and confocal Raman mappings were acquired from an Aramis confocal microscope (Horiba Jobin Yvon, Edison, New Jersey) equipped with a diode-pump solid state (DSPP) laser (wavelength λ = 532 nm). The laser beam with an intensity of 0.4 mW (unless specified otherwise) was focused using a 50× objective (NA 0.75) onto the nanofelt on a glass slides, which was further mounted onto a 200 × 200 × 200 μm piezo scanner. The Raman signals were collected with the same objective under a 180° backscattering configuration and passed through an edge filter into a monochromator and electric-cooled charge-coupled camera. The Raman spectra were collected for 1 s at each location, and Raman maps were obtained on the same confocal microscope according to a reported method.[36] All of the Raman spectra reported herein consisted of an average of six spectra, which were collected at six different locations with size of 15 × 15 μm over the samples.

2.6. Sample Evaluations. Prior to the SERS evaluation of 4-MBA, predetermined amounts of 4-MBA were dissolved into ethanol to make the 4-MBA solutions at different concentrations. Thereafter, the nanofelts of neat TiO_2, TiO_2/Ag-1 min, TiO_2/Ag-3 min, TiO_2/Ag-10 min, and TiO_2/Ag-20 min were first treated with 10^{-3} M 4-MBA solution for 3 h before acquiring the Raman map intensities; note that the soaking time (in 4-MBA solution) was set as 3 h for the subsequent experiment. Additionally, the Raman map intensity of TiO_2/Ag-10 min nanofelt was also acquired as a function of 4-MBA concentration; while the concentration of 4-MBA solutions varied from 1.0×10^{-7} to 1.0×10^{-3} M. According to the testing results, the nanofelt of TiO_2/Ag-10 min and the concentration of 10^{-5} M 4-MBA were selected to evaluate the UV-cleanable property. During the studies, the TiO_2/Ag-10 min nanofelt was first treated with 10^{-5} M 4-MBA solution (denoted hereafter as TiO_2/Ag-10 min-4-MBA); this was then followed by the measurements of Raman intensity and SERS maps. Subsequently, the TiO_2/Ag-10 min-4-MBA nanofelt was placed in a quartz vessel containing O_2-saturated water; and the system was exposed to UV irradiation for 5 h. The UV source was a 125 W high-pressure mercury lamp with intensity of 90 mW/cm^2. After the UV irradiation, the nanofelt was dried in air and performed for another SERS test. The two SERS tests (one for TiO_2/Ag-10 min-4-MBA nanofelt before UV irradiation, the other for TiO_2/Ag-10 min-4-MBA nanofelt after UV irradiation) completed one test cycle of UV-cleanable property. To further test the reproducible/reliable property, five entire cycles of SERS test for the TiO_2/Ag-10 min nanofelt were performed by loading of 4-MBA and treating with UV irradiation in O_2-saturated water alternately for 5 times. For comparison, SERS tests

dx.doi.org/10.1021/am5005859 | ACS Appl. Mater. Interfaces 2014, 6, 5759−5767

were also performed for the TiO_2/Ag-10 min nanofelt upon 4-MBA loading and O_2-saturated water treatment in dark room alternatively.

Additionally, the SERS evaluations of R6G and 4-ATP were also conducted, and the nanofelt of TiO_2/Ag-10 min and the concentration of 10^{-5} M (of R6G and 4-ATP) were selected to evaluate the UV-cleanable property. In specific, the TiO_2/Ag-10 min nanofelt was first treated with 10^{-5} M R6G or 4-ATP solution for 3 h (denoted hereafter as TiO_2/Ag-10 min-R6G and TiO_2/Ag-10 min-4-ATP, respectively); and then the Raman intensity and SERS maps were measured. Subsequently, TiO_2/Ag-10 min-R6G or TiO_2/Ag-10 min-4-ATP nanofelt was placed in a quartz vessel containing O_2-saturated water, and the system was exposed to UV irradiation for 5 h. After the UV irradiation, the nanofelt was dried in air, treated with 10^{-5} M R6G or 4-ATP, and followed by another SERS test.

3. RESULTS AND DISCUSSION

3.1. Preparation and Characterization of TiO_2 Nanofelts Surface-Decorated with Ag NPs. Upon the electroless plating for decoration of Ag NPs, a series of TiO_2 nanofelts with various growing periods of Ag NPs (i.e., 1, 3, 10, and 20 min) were prepared. The −OH groups on the surface of TiO_2 nanofelts acted as active sites for adsorption of Ag^+ ions; while the Ag^+ ions were reduced to elemental Ag, and the dextrose molecules (D−CHO) were oxidized to species containing carboxyl/carboxylate; hence, a moderately strong bond between the Ti−O− group and elemental Ag would be formed on the surface of TiO_2 nanofibers.[37,38] The morphology of electrospun TiO_2 nanofelt is shown in Figure 2A, and the TiO_2 nanofibers had the cylindrical shape with diameters of ∼200 nm; as indicated in a previous study that, the electrospun TiO_2 nanofibers were polycrystalline with crystallites (grains) having sizes of ∼10 nm.[39] The morphologies of TiO_2/Ag-1 min, TiO_2/Ag-3 min, TiO_2/Ag-10 min, and TiO_2/Ag-20 min nanofelts are shown in Figure 2B−E, respectively. When the growing/decoration time was 1 min, Ag NPs were hard to be identified on the TiO_2 nanofibers (Figure 2B). The sample with decoration time of 3 min clearly showed that numerous Ag NPs were randomly distributed on the TiO_2 nanofibers, and these Ag NPs tended to possess the spherical/ellipsoidal shape (Figure 2C).[37,38] With further prolonging the decoration time to 10 min, the Ag NPs became larger and the distances among Ag NPs were smaller (Figure 2D). When the decoration time was 20 min, the Ag NPs appeared polyhedral in morphological structure and the nanoparticles tended to grow together; this would result in the reduction of interparticle distances/gaps (Figure 2E). The TEM images (Figure 2F and Figure S1 in the Supporting Information) further depicted the morphological structure of TiO_2/Ag-10 min nanofelt, in which Ag NPs were randomly distributed on the nanofiber surfaces. The interplanar spacing (i.e., *d*-spacing) of Ag crystallites was measured as ∼2.3 Å; this was consistent with the reported value of the {111} crystallographic plane of cubic Ag.[40] The inset in Figure 1F shows a typical electron diffraction pattern acquired from TiO_2/Ag-10 min nanofelt, the diffraction dots/spots originated from silver crystals could be clearly identified, while the ring-like diffraction pattern indicated that the Ag NPs were randomly decorated on the surface of TiO_2/Ag-10 min nanofelt without particular orientation. It was also evident that adjacent Ag NPs were separated with nanoscale gaps, and these interparticle gaps would lead to the generation of Raman "hot spots", which could substantially enhance the local electromagnetic fields, resulting in enormously strong SERS activity/sensitivity.[41,42]

To further confirm the presence of Ag NPs on the surface of TiO_2 nanofelts, the energy dispersive spectroscopy (EDS) analyses were carried out for the nanofelts of TiO_2, TiO_2/Ag-1 min, TiO_2/Ag-3 min, TiO_2/Ag-10 min, and TiO_2/Ag-20 min. The EDS spectrum of TiO_2 nanofelt merely showed the peaks of Ti and O (inset in Figure 2A). On the other hand, as depicted in the insets of Figure 2B−E, the EDS spectra showed the peaks of Ti and O, as well as the peaks of Ag, indicating that Ag NPs were successfully decorated on these TiO_2 nanofelts. The EDS results also indicated that the loading amount of Ag was increased as the decoration period of Ag NPs was prolonged from 1 to 20 min.

As shown in Figure 3, the XRD pattern acquired from electrospun TiO_2 nanofelt had strong diffraction peaks centered

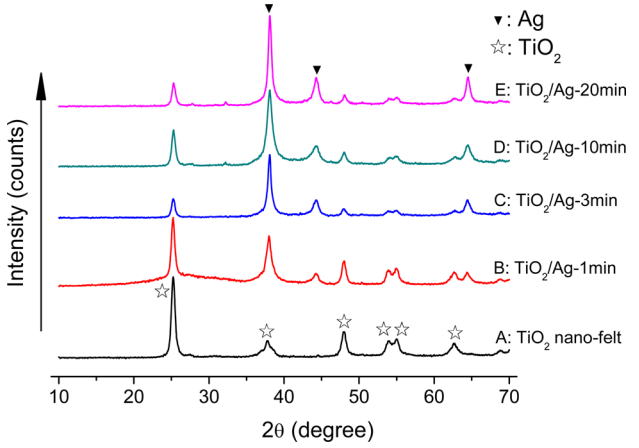

Figure 3. XRD patterns acquired from the nanofelts of TiO_2 (A), TiO_2/Ag-1 min (B), TiO_2/Ag-3 min (C), TiO_2/Ag-10 min (D), and TiO_2/Ag-20 min (E). The XRD patterns are offset arbitrarily for ease of presentation.

at 2θ values of 25.2°, 37.8°, 48.0°, 53.9°, 55.1°, and 62.7° (curve A), which could be assigned to the {101}, {004}, {200}, {105}, {211}, and {204} crystallographic planes of (tetragonal) anatase-phase TiO_2, respectively.[43,44] The XRD patterns of TiO_2/Ag nanofelts (curve B, C, D, and E) exhibited three additional diffraction peaks centered at 38.2°, 44.2°, and 64.5°, which could be assigned to the {111}, {200}, and {220} crystallographic planes of cubic crystal structure of elemental silver, respectively.[45] As the growing period of Ag NPs increased from 1 to 20 min, the diffraction peaks of Ag became stronger, indicating higher silver density on the surface of TiO_2/Ag nanofelts. The XRD results further confirmed the presence of both Ag NPs and anatase-phase TiO_2 in the resulting TiO_2/Ag nanofelts, and such results were in agreement with those acquired from SEM and TEM analyses (insets in Figure 2B−2E).

3.2. SERS Evaluation of TiO_2 Nanofelts Surface-Decorated with Ag NPs. *3.2.1. SERS Evaluation by Using 4-MBA as the Probe Analyte.* During the evaluation, the Raman map intensity was acquired by tracing the Raman peak centered at 1580 cm^{-1}, and all of the Raman spectra reported herein consisted of an average of six spectra, which were collected at six different locations with size of 15 × 15 μm over the nanofelts arbitrarily. The SERS activity/sensitivity of neat TiO_2, TiO_2/Ag-1 min, TiO_2/Ag-3 min, TiO_2/Ag-10 min, and TiO_2/Ag-20 min nanofelts was studied by using 4-MBA as the probe analyte. Figure 4A shows the average Raman intensities

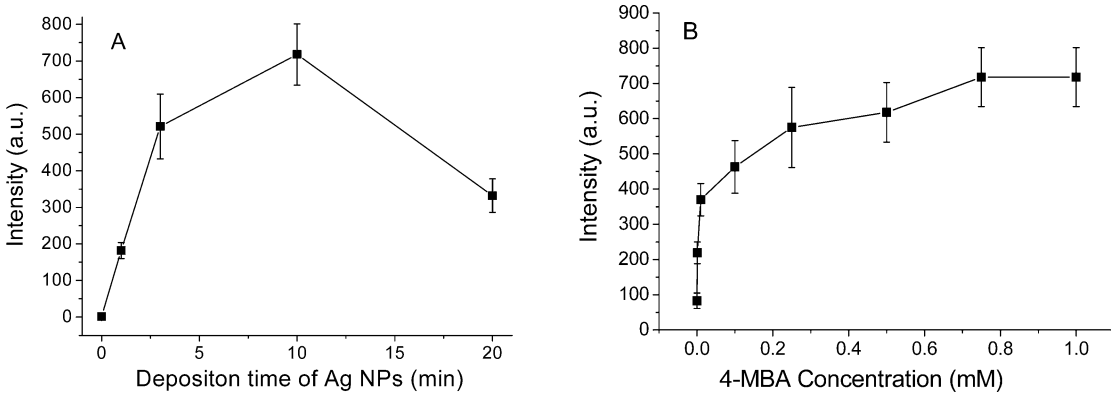

Figure 4. (A) Raman map intensities of neat TiO_2, TiO_2/Ag-1 min, TiO_2/Ag-3 min, TiO_2/Ag-10 min, and TiO_2/Ag-20 min nanofelts (after being treated with 10^{-3} M 4-MBA solution). (B) Raman map intensity of TiO_2/Ag-10 min nanofelt versus 4-MBA concentration. The Raman map intensity was acquired by tracing the Raman peak centered at 1580 cm^{-1}. Each datum is the average value of six different locations/positions with size of 15 × 15 μm over the sample, while an error bar shows one standard deviation.

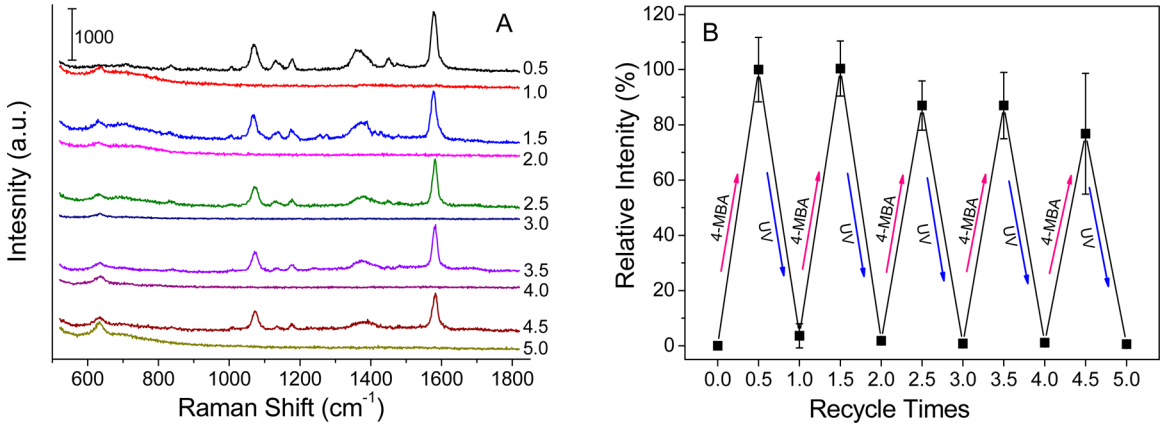

Figure 5. (A) Raman spectra acquired from the TiO_2/Ag-10 min nanofelt with 5 repeated loadings of 4-MBA and 5 repeated treatments with UV irradiation alternately; the spectra are arbitrarily offset for ease of presentation. (B) SERS responses (traced by using the map intensity from the Raman peak centered at 1580 cm^{-1}) of the TiO_2/Ag-10 min nanofelt upon 5 repeated loadings of 4-MBA and 5 repeated treatments with UV irradiation alternately.

as a function of electroless plating time for different TiO_2/Ag nanofelts (the corresponding Raman spectra are shown in Figure S2 in the Supporting Information). It was evident that, the Raman signal of neat TiO_2 was merely 1.57 ± 8.19 (Supporting Information Figure S3), and the strongest Raman signals were obtained from the TiO_2 nanofelt with decoration time of 10 min. The appearance of strong Raman signals in TiO_2/Ag-10 min was in consistence with the TEM result in Figure 2F; that is, the Ag NPs were separated with nanoscale gaps, and these interparticle gaps would lead to the generation of Raman "hot spots", which could substantially enhance the local electromagnetic fields, resulting in enormously strong SERS activity/sensitivity.[41,42] As indicated in the Supporting Information, the enhancement factor (EF) of TiO_2/Ag-10 min reached 5.62 × 10^6. Figure 4B demonstrates the Raman intensity as a function of 4-MBA concentration for the TiO_2/Ag-10 min nanofelt (the corresponding Raman spectra are shown in Supporting Information Figure S4). The SERS intensity was at 82.6 (arbitrary unit) when the 4-MBA concentration was at 1.0 × 10^{-7} mol/L (~15 ppb), this detectable concentration of 4-MBA (i.e., 15 ppb) was comparable to other electrospun nanofiber/Ag based SERS substrates (10 ppb);[35] and then the SERS intensity would be increased rapidly with the increase of 4-MBA concentration. When the 4-MBA concentration was at 1.0 × 10^{-5} mol/L, the SERS intensity reached 370. With further increase of 4-MBA concentration, the increase of SERS intensity became less significant. This could be attributed to the saturation of 4-MBA molecules on the surface of TiO_2/Ag-10 min nanofelt, and the acquired concentration-dependent results were similar to those reported in literature.[46] According to the results from the above two tests, the nanofelt of TiO_2/Ag-10 min and the 4-MBA concentration of 10^{-5} mol/L were selected to evaluated the UV-cleanable property.

To test the UV-cleanable property, the TiO_2/Ag-10 min nanofelt was first immersed in 10^{-5} M 4-MBA aqueous solution; the Raman map intensity was then measured. Thereafter, the TiO_2/Ag-10 min-4-MBA nanofelt was placed in O_2-saturated water under UV irradiation for 5 h. After that, the nanofelt was dried in air followed by another SERS test. Note that 5 entire cycles of SERS test for the TiO_2/Ag-10 min nanofelt were carried out by 5 repeated loadings of 4-MBA and 5 repeated treatments with UV irradiation alternately. For ease of presentation, the curves of 0.5, 1.5, 2.5, 3.5, and 4.5 in Figure 5 represented SERS tests for the TiO_2/Ag-10 min nanofelt after being treated with 4-MBA, while the curves of 1.0, 2.0, 3.0, 4.0, and 5.0 represented SERS tests of the TiO_2/Ag-10 min nanofelt after the treatment with UV irradiation in O_2-saturated water.

dx.doi.org/10.1021/am5005859 | ACS Appl. Mater. Interfaces 2014, 6, 5759−5767

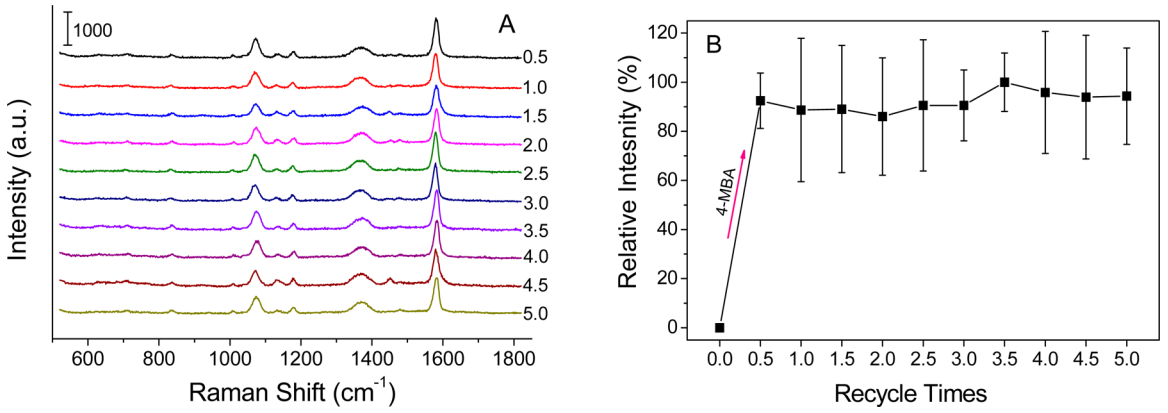

Figure 6. (A) Raman spectra of the TiO_2/Ag-10 min nanofelt with 5 repeated loadings of 4-MBA and 5 repeated treatments with O_2-saturated water in dark room alternately; the spectra are offset arbitrarily for ease of presentation. (B) SERS responses (traced by using the map intensity from the Raman peak centered at 1580 cm^{-1}) of the TiO_2/Ag-10 min nanofelt upon 5 repeated loadings of 4-MBA and 5 repeated treatments with O_2-saturated water in dark room alternately.

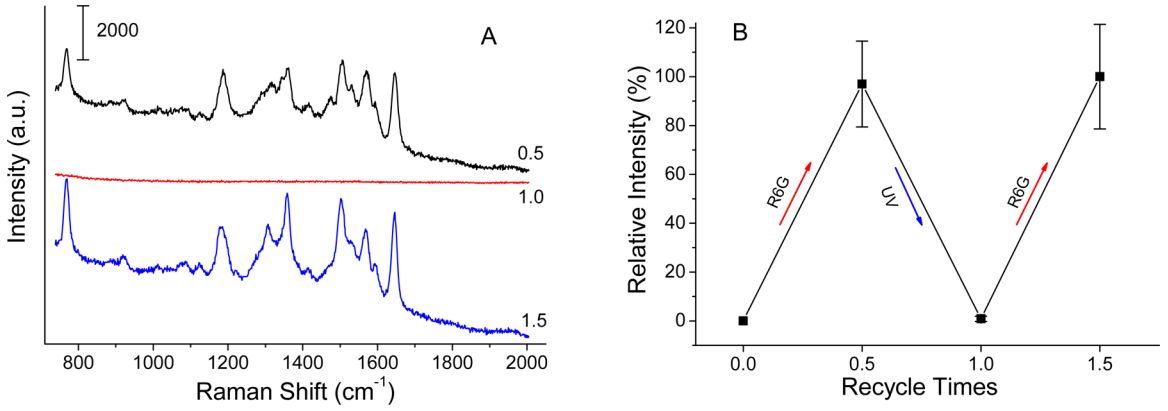

Figure 7. (A) Raman spectra acquired from the TiO_2/Ag-10 min nanofelt with 2 repeated loadings of R6G and one treatment with UV irradiation alternately; the spectra are arbitrarily offset for ease of presentation. (B) SERS responses (traced by using the map intensity from the Raman bands in the range of 1440−1620 cm^{-1}) of the TiO_2/Ag-10 min nanofelt upon 2 repeated loadings of R6G and one treatment with UV irradiation alternately.

As shown in the spectra (Figure 5A), the Raman peaks of TiO_2/Ag-10 min-4-MBA (the curves of 0.5, 1.5, 2.5, 3.5, and 4.5) were centered at 630, 1071, 1132, 1178, 1371, and 1579 cm^{-1}. The Raman band at 630 cm^{-1} was attributed to the Raman scattering of anatase TiO_2,[47] while the rest bands were in consistence with the Raman signals of the adsorbed 4-MBA molecules.[46,48] However, such SERS signals completely disappeared for the TiO_2/Ag-10 min nanofelt after being treated with UV irradiation in O_2-saturated water (the curves of 1.0, 2.0, 3.0, 4.0, and 5.0). As shown in Figure 5B, the relative intensity dropped to zero after each UV irradiation; meanwhile, after 5 repeated loadings of 4-MBA, the relative intensity still remained at ~80% level. As shown in Supporting Information Figure S6, the Ag NPs still retained after 5 repeated loadings of 4-MBA and 5 repeated treatments with UV irradiations alternately; moreover, as indicated in Figure S7 and S8 (all of data were acquired from the TiO_2/Ag-10 min sample after five 4-MBA loadings and four UV irradiations alternately), the Raman signals could be observed at any location across the typical examined area (Supporting InformationFigure S7), and the histogram of Raman intensity (acquired from six different areas arbitrarily) was very uniform (Figure S8). The above results demonstrated the excellent UV-cleanable property and reproducibility/reliability of TiO_2/Ag-10 min SERS-active substrate. These results clearly indicated that, the combination of UV irradiation with O_2-saturated water was very effective for cleaning/removing of organic compounds (4-MBA in this case) from TiO_2/Ag nanofelts; and this was due to catalytic property of anatase-phase TiO_2 toward photodegradation of organic compounds. As TiO_2 irradiated under UV light, the photodegradation typically starts with the reduction of dissolved/adsorbed molecular oxygen into a superoxide radical, which will then generate highly active oxidative species such as $^{\bullet}O_2^-$ and $^{\bullet}OH$; these oxidative species can subsequently lead to the degradation of organic compounds adsorbed on the surfaces of TiO_2/Ag nanofelts.[22−25]

To determine whether O_2-saturated water alone could clean (i.e., remove 4-MBA molecules from) the TiO_2/Ag-10 min nanofelt, the nanofelt was first immersed in 10^{-5} M 4-MBA solution; the Raman map intensity was then measured. Thereafter, the TiO_2/Ag-10 min-4-MBA nanofelt was placed into O_2-saturated water in dark room for 5 h (without UV irradiation) followed by another measurement of Raman map intensity. Note that 5 entire cycles of SERS test were carried out for the TiO_2/Ag-10 min nanofelt by 5 repeated loadings of 4-MBA and 5 repeated treatments with O_2-saturated water in dark room alternately. For ease of presentation, the curves of 0.5, 1.5, 2.5, 3.5, and 4.5 in Figure 6 represented SERS tests for the TiO_2/Ag-10 min nanofelt after being treated with 10^{-5} M 4-MBA, while the curves of 1.0, 2.0, 3.0, 4.0, and 5.0

dx.doi.org/10.1021/am5005859 | ACS Appl. Mater. Interfaces 2014, 6, 5759−5767

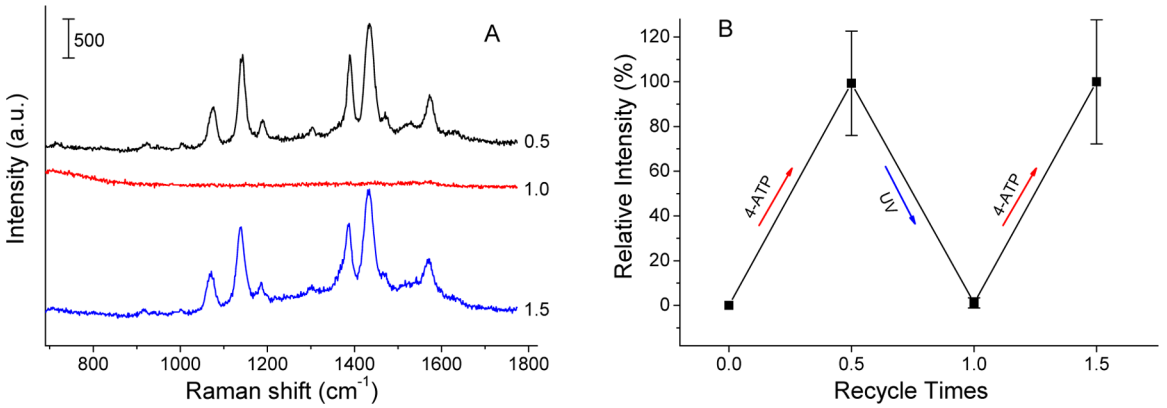

Figure 8. (A) Raman spectra acquired from the TiO_2/Ag-10 min nanofelt with 2 repeated loadings of 4-ATP and one treatment with UV irradiation alternately; the spectra are arbitrarily offset for ease of presentation. (B) SERS responses (traced by using the map intensity from the Raman peak centered at 1435 cm^{-1}) of the TiO_2/Ag-10 min nanofelt upon 2 repeated loadings of 4-ATP and one treatment with UV irradiation alternately.

represented the SERS tests for the same nanofelt after the treatment with O_2-saturated water in dark room for 5 h. As shown in Figure 6A, the Raman peaks of TiO_2/Ag-10 min nanofelt with 4-MBA (the curves of 0.5, 1.5, 2.5, 3.5, and 4.5) were centered at 1071, 1132, 1178, 1371, and 1579 cm^{-1}, which were in consistence with the Raman signals of adsorbed 4-MBA.[45,46] Without the use of UV irradiation, no appreciable change in SERS spectra could be identified after the treatment in O_2-saturated water for 5 h (Figure 6B), indicating that the UV irradiation would be necessary for the regeneration of SERS-active substrate of TiO_2/Ag nanofelts.

3.2.2. SERS Evaluation by Using R6G and 4-ATP as the Probe Analytes. R6G and 4-ATP were also selected as the target analytes to further test the UV-cleanable property of TiO_2/Ag-10 min nanofelt. During the evaluation, the TiO_2/Ag-10 min nanofelt was first treated with 10^{-5} M R6G or 4-ATP solution, the Raman intensity and SERS maps were then measured. Subsequently, TiO_2/Ag-10 min-R6G or TiO_2/Ag-10 min-4-ATP nanofelt was placed in a quartz vessel containing O_2-saturated water under UV irradiation for 5 h. After the UV irradiation, the nanofelt was dried in air, treated with 10^{-5} M R6G or 4-ATP, and followed by another SERS test. For ease of presentation, the curves of 0.5 and 1.5 in Figure 7A and 8A represented SERS tests for the TiO_2/Ag-10 min nanofelt after being treated with R6G or 4-ATP, while the curves of 1.0 represented SERS test of the TiO_2/Ag-10 min nanofelt after being irradiated with UV in O_2-saturated water.

As shown in Figure 7A, the Raman peaks of TiO_2/Ag-10 min-R6G (the curves of 0.5 and 1.5) were centered at 769, 1182, 1307, 1360, 1506, 1570, and 1650 cm^{-1}, which were in consistence with the Raman signals of the adsorbed R6G molecules.[35] However, such SERS signals completely disappeared for the TiO_2/Ag-10 min nanofelt after being treated with UV irradiation in O_2-saturated water (the curves of 1.0). As shown in Figure 7B, the relative intensity dropped to zero after the UV irradiation; meanwhile, after the R6G loading, the relative intensity recovered back to ~100%. The above results clearly demonstrated the excellent UV-cleanable property and reproducibility/reliability of TiO_2/Ag-10 min SERS-active substrate.

As shown in Figure 8A, the Raman peaks of TiO_2/Ag-10 min-4-ATP (the curves of 0.5 and 1.5) were centered at 1075, 1143, 1189, 1506, 1389, 1434, and 1575 cm^{-1}, which were in consistence with the Raman signals of the adsorbed 4-ATP molecules.[49] However, such SERS signals completely disappeared for the TiO_2/Ag-10 min nanofelt after being treated with UV irradiation in O_2-saturated water (the curves of 1.0). As shown in Figure 8B, the relative intensity dropped to zero after the UV irradiation; meanwhile, after the 4-ATP loading, the relative intensity returned to ~100%. The above results once again demonstrated the excellent UV-cleanable property and reproducibility/reliability of TiO_2/Ag-10 min SERS-active substrate. The results in Figures 7 and 8 further indicated that, the combination of UV irradiation with O_2-saturated water was very effective for cleaning/removing the target analytes (i.e., 4-MBA, R6G, and 4-ATP) from TiO_2/Ag nanofelts; and this was due to catalytic property of anatase-phase TiO_2 toward photodegradation of organic compounds.

In summary, the TiO_2/Ag-10 min nanofelt could be cleaned easily and effectively upon UV irradiation in O_2-saturated water, which would make the TiO_2/Ag nanofelt promising as highly sensitive, cost-effective, and reproducible/reliable substrate for a variety of SERS applications.

4. CONCLUSIONS

The electrospun nanofelt consisting of anatase-phase TiO_2 nanofibers with diameters of ~200 nm was prepared, and the nanofelt was then surface-decorated with Ag NPs via the electroless plating method. The SERS activity/sensitivity of TiO_2/Ag nanofelt was studied by using 4-MBA, R6G, and 4-ATP as the probe analytes, and the UV-cleanable property was studied as well. The results indicated that the TiO_2/Ag-10 min nanofelt exhibited the highest SERS activity/sensitivity, and it could be cleaned and regenerated/recovered upon UV irradiation in O_2-saturated water due to high photodegradation property of anatase-phase TiO_2. This study suggested that electrospun TiO_2/Ag nanofelt would be promising as SERS-active substrate with UV-cleanable property for cost-effective and reproducible/reliable SERS applications.

■ ASSOCIATED CONTENT

Supporting Information

Figures showing representative TEM images, Raman spectra, histograms, representative SEM images, and Raman maps and additional discussion. This material is available free of charge via the Internet at http://pubs.acs.org.

AUTHOR INFORMATION

Corresponding Authors

*Tel.: (605) 677-6250. Fax: (605) 677-6397. E-mail: Chaoyang.Jiang@usd.edu.

*Tel.: (605) 394-1229. Fax: (605) 394-1232. E-mail: Hao.Fong@sdsmt.edu.

Author Contributions

Y.Z. and L.S. contributed equally to this work.

Notes

The authors declare no competing financial interest.

ACKNOWLEDGMENTS

This research was supported by the National Aeronautics and Space Administration (Cooperative Agreement No. NNX10A-N34A), the National Science Foundation (Grant No. EPS-0903804), and the State of South Dakota.

REFERENCES

(1) Nie, S. M.; Emery, S. R. Probing Single Molecules and Single Nanoparticles by Surface-Enhanced Raman Scattering. *Science* **1997**, *275*, 1102−1106.

(2) Chang, C. C.; Yang, K. H.; Liu, Y. C.; Hsu, T. C.; Mai, F. D. Surface-Enhanced Raman Scattering-Active Au/SiO_2 Nanocomposites Prepared Using Sonoelectrochemical Pulse Deposition Methods. *ACS Appl. Mater. Interfaces* **2012**, *4*, 4700−4707.

(3) Kleinman, S. L.; Ringe, E.; Valley, N.; Wustholz, K. L.; Phillips, E.; Scheidt, K. A.; Schatz, G. C.; Van Duyne, R. P. Single-Molecule Surface-Enhanced Raman Spectroscopy of Crystal Violet Isotopologues: Theory and Experiment. *J. Am. Chem. Soc.* **2011**, *133*, 4115−4122.

(4) Liang, H. Y.; Li, Z. P.; Wang, W. Z.; Wu, Y. S.; Xu, H. X. Highly Surface-Roughened "Flower-Like" Silver Nanoparticles for Extremely Sensitive Substrates of Surface-Enhanced Raman Scattering. *Adv. Mater.* **2009**, *21*, 4614−4618.

(5) Gandra, N.; Singamaneni, S. Bilayered Raman-Intense Gold Nanostructures with Hidden Tags (BRIGHTs) for High-Resolution Bioimaging. *Adv. Mater.* **2013**, *25*, 1022−1027.

(6) Guo, B.; Han, G. Y.; Li, M. Y.; Zhao, S. Z. Deposition of the Fractal-Like Gold Particles onto Electrospun Polymethylmethacrylate Fibrous Mats and Their Application in Surface-Enhanced Raman Scattering. *Thin Solid Films* **2010**, *518*, 3228−3233.

(7) Banholzer, M. J.; Millstone, J. E.; Qin, L.; Mirkin, C. A. Rationally Designed Nanostructures for Surface-Enhanced Raman Spectroscopy. *Chem. Soc. Rev.* **2008**, *37*, 885−897.

(8) Wang, H.; Halas, N. J. Mesoscopic Au "Meatball" Particles. *Adv. Mater.* **2008**, *20*, 820−825.

(9) Ko, H.; Chang, S.; Tsukruk, V. V. Porous Substrates for Label-Free Molecular Level Detection of Nonresonant Organic Molecules. *ACS Nano* **2009**, *3*, 181−188.

(10) Zhai, Y.; Zhai, J.; Wang, Y.; Guo, S.; Ren, W.; Dong, S. Fabrication of Iron Oxide Core/Gold Shell Submicrometer Spheres with Nanoscale Surface Roughness for Efficient Surface-Enhanced Raman Scattering. *J. Phys. Chem. C* **2009**, *113*, 7009−7014.

(11) Zhang, Z.; Xu, F.; Yang, W.; Guo, M.; Wang, X.; Zhang, B.; Tang, J. A Facile One-Pot Method to High-Quality Ag-Graphene Composite Nanosheets for Efficient Surface-Enhanced Raman Scattering. *Chem. Commun.* **2011**, *47*, 6440−6442.

(12) Dzenis, Y. Spinning Continuous Fibers for Nanotechnology. *Science* **2004**, *304*, 1917−1919.

(13) Greiner, A.; Wendorff, J. H. Electrospinning: A Fascinating Method for the Preparation of Ultrathin Fibres. *Angew. Chem., Int. Ed.* **2007**, *46*, 5670−5703.

(14) Carlberg, B.; Ye, L. L.; Liu, J. H. Surface-Confined Synthesis of Silver Nanoparticle Composite Coating on Electrospun Polyimide Nanofibers. *Small* **2011**, *7*, 3057−3066.

(15) Guo, B.; Zhao, S. Z.; Han, G. Y.; Zhang, L. W. Continuous Thin Gold Films Electroless Deposited on Fibrous Mats of Polyacrylonitrile and Their Electrocatalytic Activity Towards the Oxidation of Methanol. *Electrochim. Acta* **2008**, *53*, 5174−5179.

(16) Ochanda, F.; Jones, W. E. Fabrication and Thermal Analysis of Submicron Silver Tubes Prepared from Electrospun Fiber Templates. *Langmuir* **2007**, *23*, 795−801.

(17) He, D.; Hu, B.; Yao, Q. F.; Wang, K.; Yu, S. H. Large-Scale Synthesis of Flexible Free-Standing SERS Substrates with High Sensitivity: Electrospun PVA Nanofibers Embedded with Controlled Alignment of Silver Nanoparticles. *ACS Nano* **2009**, *3*, 3993−4002.

(18) Zhang, C. L.; Lv, K. P.; Cong, H. P.; Yu, S. H. Controlled Assemblies of Gold Nanorods in PVA Nanofiber Matrix as Flexible Free-Standing SERS Substrates by Electrospinning. *Small* **2012**, *8*, 648−653.

(19) Cao, M.; Cheng, S.; Zhou, X.; Tao, Z.; Yao, J.; Fan, L. J. Preparation and Surface-Enhanced Raman Performance of Electrospun Poly(Vinyl Alcohol)/ High-Concentration-Gold Nanofibers. *J. Polym. Res.* **2012**, *19*, 1−7.

(20) Lee, C. H.; Tian, L.; Abbas, A.; Kattumenu, R.; Singamaneni, S. Directed Assembly of Gold Nanorods Using Aligned Electrospun Polymer Nanofibers for Highly Efficient SERS Substrates. *Nanotechnology* **2012**, *4*, No. 275311.

(21) Diebold, U. The Surface Science of Titanium Dioxide. *Surf. Sci. Rep.* **2003**, *48*, 53−229.

(22) Anipsitakis, G. P.; Dionysiou, D. D. Transition Metal/UV-Based Advanced Oxidation Technologies for Water Decontamination. *Appl. Catal., B* **2004**, *54*, 155−163.

(23) Krysa, J.; Jirkovsky, J. Electrochemically Assisted Photocatalytic Degradation of Oxalic Acid on Particulate TiO_2 Film in a Batch Mode Plate Photoreactor. *J. Appl. Electrochem.* **2002**, *32*, 591−596.

(24) Zhang, Z.; Yu, Y.; Wang, P. Hierarchical Top-Porous/Bottom-Tubular TiO_2 Nanostructures Decorated with Pd Nanoparticles for Efficient Photoelectrocatalytic Decomposition of Synergistic Pollutants. *ACS Appl. Mater. Interfaces* **2012**, *4*, 990−996.

(25) Houas, A.; Lachheb, H.; Ksibi, M.; Elaloui, E.; Guillard, C.; Herrmann, J. M. Degradation Pathway of Methylene Blue in Water. *Appl. Catal., B* **2001**, *31*, 145−157.

(26) Liu, L.; Gu, X.; Ji, Z.; Zou, W.; Tang, C.; Gao, F.; Dong, L. Anion-Assisted Synthesis of TiO_2 Nanocrystals with Tunable Crystal Forms and Crystal Facets and Their Photocatalytic Redox Activities in Organic Reactions. *J. Phys. Chem. C* **2013**, *117*, 18578−18587.

(27) Tachikawa, T.; Yamashita, S.; Majima, T. Evidence for Crystal-Face-Dependent TiO_2 Photocatalysis from Single-Molecule Imaging and Kinetic Analysis. *J. Am. Chem. Soc.* **2011**, *133*, 7197−7204.

(28) Li, X.; Chen, G.; Yang, L.; Jin, Z.; Liu, J. Multifunctional Au-Coated TiO_2 Nanotube Arrays as Recyclable SERS Substrates for Multifold Organic Pollutants Detection. *Adv. Funct. Mater.* **2010**, *20*, 2815−2824.

(29) Li, X.; Hu, H.; Li, D.; Shen, Z.; Xiong, Q.; Li, S.; Fan, H. J. Ordered Array of Gold Semishells on TiO_2 Spheres: An Ultrasensitive and Recyclable SERS Substrate. *ACS Appl. Mater. Interfaces* **2012**, *4*, 2180−2185.

(30) Zou, X.; Silva, R.; Huang, X.; Asefa, T. A Self-Cleaning porous TiO_2-Ag Core-Shell Nanocomposite Material for Surface-Enhanced Raman Scattering. *Chem. Commun.* **2013**, *49*, 382−384.

(31) Fu, X.; Zhang, G.; Wu, T.; Wang, S. Multifunctional Gold-Loaded TiO_2 Thin Film: Photocatalyst and Recyclable SERS Substrate. *Can. J. Chem.* **2013**, *91*, 1112−1116.

(32) Yang, X.; Zhong, H.; Zhu, Y.; Shen, J.; Li, C. Ultrasensitive and Recyclable SERS Substrate Based on Au-Decorated Si Nanowire Arrays. *Dalton Trans.* **2013**, *42*, 14324−14330.

(33) Kassu, A.; Sharma, A.; Ruffin, P.; Sadate, S.; Calzzani, F.; Brantley, C.; Edwards, E. Recycling of Surface-Enhanced Raman Substrates by Ultraviolet Cleaning. *Opt. Eng.* **2010**, *49*, 106501−106504.

(34) Sirimuthu, N. M.; Syme, C. D.; Cooper, J. M. Investigation of the Stability of Labelled Nanoparticles for SE(R)RS Measurements in Cells. *Chem. Commun.* **2011**, *47*, 4099−4101.

(35) Zhang, L.; Gong, X.; Bao, Y.; Zhao, Y.; Xi, M.; Jiang, C.; Fong, H. Electrospun Nanofibrous Membranes Surface-Decorated with Silver Nanoparticles as Flexible and Active/Sensitive Substrates for Surface-Enhanced Raman Scattering. *Langmuir* **2012**, *28*, 14433−14440.
(36) Netzer, N. L.; Qiu, C.; Zhang, Y.; Lin, C.; Zhang, L.; Fong, H.; Jiang, C. Gold−Silver Bimetallic Porous Nanowires for Surface-Enhanced Raman Scattering. *Chem. Commun.* **2011**, *47*, 9606−9608.
(37) Ochanda, F.; Jones, W. E. Sub-Micrometer-Sized Metal Tubes from Electrospun Fiber Templates. *Langmuir* **2005**, *21*, 10791−10796.
(38) Kim, S. D.; Choe, W. G.; Jeong, J. R. Environmentally Friendly Electroless Plating for Ag/TiO_2-Coated Core-Shell Magnetic Particles Using Ultrasonic Treatment. *Ultrason. Sonochem.* **2013**, *20*, 1456−1462.
(39) He, G.; Cai, Y.; Zhao, Y.; Wang, W.; Lai, C.; Xi, M.; Zhu, Z.; Fong, H. Electrospun Anatase-Phase TiO_2 Nanofibers with Different Morphological Structures and Specific Surface Areas. *J. Colloid Interface Sci.* **2013**, *398*, 103−111.
(40) Ding, X.; Briggs, G.; Zhou, W.; Chen, Q.; Peng, L. M. In Situ Growth and Characterization of Ag and Cu Nanowires. *Nanotechnology* **2006**, *17*, S376−S380.
(41) Hao, E.; Schatz, G. C. Electromagnetic Fields around Silver Nanoparticles and Dimers. *J. Chem. Phys.* **2004**, *120*, 357−366.
(42) Canamares, M. V.; Garcia-Ramos, J. V.; Gomez-Varga, J. D.; Domingo, C.; Sanchez-Cortes, S. Comparative Study of the Morphology, Aggregation, Adherence to Glass, and Surface-Enhanced Raman Scattering Activity of Silver Nanoparticles Prepared by Chemical Reduction of Ag^+ Using Citrate and Hydroxylamine. *Langmuir* **2005**, *21*, 8546−8553.
(43) He, G.; Wang, X.; Xi, M.; Zheng, F.; Zhu, Z.; Fong, H. Fabrication and Evaluation of Dye-Sensitized Solar Cells with Photoanodes Based on Electrospun TiO_2 Nanotubes. *Mater. Lett.* **2013**, *106*, 115−118.
(44) Beuvier, T.; Richard-Plouet, M.; Brohan, L. Accurate Methods for Quantifying the Relative Ratio of Anatase and TiO_2(B) Nanoparticles. *J. Phys. Chem. C* **2009**, *113*, 13703−13706.
(45) Barakat, N. A. M.; Woo, K. D.; Kanjwal, M. A.; Choi, K. E.; Khil, M. S.; Kim, H. Y. Surface Plasmon Resonances, Optical Properties, and Electrical Conductivity Thermal Hystersis of Silver Nanofibers Produced by the Electrospinning Technique. *Langmuir* **2008**, *24*, 11982−11987.
(46) Yan, J.; Han, X.; He, J.; Kang, L.; Zhang, B.; Du, Y.; Zhao, H.; Dong, C.; Wang, H. L.; Xu, P. Highly Sensitive Surface-Enhanced Raman Spectroscopy (SERS) Platforms Based on Silver Nanostructures Fabricated on Polyaniline Membrane Surfaces. *ACS Appl. Mater. Interfaces* **2012**, *4*, 2752−2756.
(47) Kelly, S.; Pollak, F. H.; Tomkiewicz, M. Raman Spectroscopy as a Morphological Probe for TiO_2 Aerogels. *J. Phys. Chem. B* **1997**, *101*, 2730−2734.
(48) Hunyadi, S. E.; Murphy, C. J. Bimetallic Silver−Gold Nanowires: Fabrication and Use in Surface-Enhanced Raman Scattering. *J. Mater. Chem.* **2006**, *16*, 3929−3935.
(49) Gregas, M. K.; Yan, F.; Scaffidi, J.; Wang, H. N.; Vo-Dinh, T. Characterization of Nanoprobe Uptake in Single Cells: Spatial and Temporal Tracking via SERS Labeling and Modulation of Surface Charge. *Nanomedicine: NBM* **2011**, *7*, 115−122.